PROTEINS
STRUCTURE ■ FUNCTION ■ BIOINFORMATICS

Unraveling the molecular basis for ligand binding in truncated hemoglobins: The trHbO *Bacillus subtilis* case

Leonardo Boechi,[1]* Pau Arroyo Mañez,[1] F. Javier Luque,[2] Marcelo A. Marti,[1,3] and Dario A. Estrin[1]*

[1] Departamento de Química Inorgánica, Analítica y Química Física/INQUIMAE-CONICET, Facultad de Ciencias Exactas y Naturales, Universidad de Buenos Aires, Ciudad Universitaria, Pabellón 2, Buenos Aires, C1428EHA, Argentina
[2] Departament de Fisicoquímica and Institut de Biomedicina (IBUB), Facultat de Farmàcia, Universitat de Barcelona, Avenida Diagonal 643, 08028, Barcelona, Spain
[3] Departamento de Química Biológica Facultad de Ciencias Exactas y Naturales, Universidad de Buenos Aires. Ciudad Universitaria, Pabellón II, Buenos Aires (C1428EHA), Argentina

ABSTRACT

Truncated hemoglobins (trHbs) are heme proteins present in bacteria, unicellular eukaryotes, and higher plants. Their tertiary structure consists in a 2-over-2 helical sandwich, which display typically an inner tunnel/cavity system for ligand migration and/or storage. The microorganism *Bacillus subtilis* contains a peculiar trHb, which does not show an evident tunnel/cavity system connecting the protein active site with the solvent, and exhibits anyway a very high oxygen association rate. Moreover, resonant Raman results of CO bound protein, showed that a complex hydrogen bond network exists in the distal cavity, making it difficult to assign unambiguously the residues involved in the stabilization of the bound ligand. To understand these experimental results with atomistic detail, we performed classical molecular dynamics simulations of the oxy, carboxy, and deoxy proteins. The free energy profiles for ligand migration suggest that there is a key residue, GlnE11, that presents an alternate conformation, in which a wide ligand migration tunnel is formed, consistently with the kinetic data. This tunnel is topologically related to the one found in group I trHbs. On the other hand, the results for the CO and O_2 bound protein show that GlnE11 is directly involved in the stabilization of the cordinated ligand, playing a similar role as TyrB10 and TrpG8 in other trHbs. Our results not only reconcile the structural data with the kinetic information, but also provide additional insight into the general behaviour of trHbs.

Proteins 2010; 78:962–970.

Key words: truncated hemoglobin; *B. subtilis*; ligand migration; molecular dynamics.

INTRODUCTION

Truncated hemoglobins (trHbs) are a subfamily of the globin family, widely distributed among bacteria, protozoa, and plants.[1,2] Their name reflect the fact that the sequence of TrHb is shorter by 20–40 residues compared to typical globins. The function of TrHbs is in many cases poorly understood, but roles, such as O_2/NO sensors, oxygen carriers under hypoxic conditions, or pseudoenzymes have been proposed.[3–5] Phylogenetic analysis of TrHb sequences have suggested the existence of three distinct groups denoted I, II, and III (also known as N, O, and P, respectively). The group II is supposed to be the ancestor of the three.[6] Noteworthy, many organisms have more than one TrHb belonging to different groups, and some display members from all three groups. The presence of multiple TrHbs in the same organism and the fact that in many cases they also coexist with members of the common globin family suggest that different members may fulfill completely different functions.

Structural analysis has shown that the three kinds of TrHbs share the same overall folding domain. Instead of the typical 3-on-3 helix fold of common globins, as myoglobin, TrHbs are formed by a 2-on-2 helical sandwich.[2] Interestingly, many topological positions are conserved and are common to the whole globin family, such as HisF8, which coordinates the iron on the proximal site and is the only residue fully conserved in the whole family. Other topologically conserved positions are residues B10, E7, E11, and

Additional Supporting Information may be found in the online version of this article.
Grant sponsor: ANPCyT; Grant number: PICT 06-25667; Grant sponsor: Spanish Ministerio de Educación y Ciencia; Grant number: CTQ2005-08797-C02-01/BQU; Grant sponsors: CONICET, University of Buenos Aires, J. S. Guggenheim Foundation, EU FP7 program (project Nostress).
*Correspondence to: Leonardo Boechi, Departamento de Química Inorgánica, Analítica y Química Física/INQUIMAE-CONICET. E-mail: lboechi@qi.fcen.uba.ar or Dario A. Estrin, Departamento de Química Inorgánica, Analítica y Química Física/INQUIMAE-CONICET, Facultad de Ciencias Exactas y Naturales, Universidad de Buenos Aires. Ciudad Universitaria, Pabellón II, Buenos Aires (C1428EHA), Argentina. E-mail: dario@qi.fcen.uba.ar
Received 1 April 2009; Revised 11 September 2009; Accepted 15 September 2009
Published online 28 September 2009 in Wiley InterScience (www.interscience.wiley.com).
DOI: 10.1002/prot.22620

G8, which are generally responsible for protein interactions with the bound ligand. These residues usually form complex hydrogen bond networks (HB) that modulate ligand binding.[4]

One of the most striking structural feature of TrHb structures is the presence of several tunnels connecting the active site with the solvent. These tunnels have been proposed to play a key role in determining ligand migration through the protein matrix.[1] This proposal is based on the fact that ligand association rate constants are determined by both accessibility of ligand to the active site and coordination to the iron, but the former is usually the rate limiting step.[7]

The most studied trHbs are probably *Mycobacterium tuberculosis Mt*-TrHbO and *Mt*-TrHbN. In *Mt*-trHbO a tight and complex hydrogen bond (HB) network is formed by the distal residues TrpG8, TyrB10, and TyrCD1 [Fig. 1(a)]. The TrpG8 is mainly responsible for the strong interaction with the bound oxygen, resulting in a very low dissociation rate and therefore high oxygen affinity. In *Mt*-trHbN the distal HB network formed by TyrB10 and GlnE11 contributes to the low dissociation rate constants (*koff*) compared to myoglobin. However, the absence of TrpG8 may explain the increase in *koff* compared to *Mt*-trHbO.[8,9] Moreover, in *Mt*-trHbN O_2 binding alters the HB network that leads to a conformational change, which in turn causes an alteration in the ligand migration, allowing a efficient NO detoxification.[10,11]

All members of the group N studied so far show the presence of a long tunnel (LT) parallel to the long protein axis, topologically positioned towards helices B and E. Two short tunnels roughly normal to the LT are also found. The first can be described as the one found in *Mt*-TrHbN, next to key residues ValG8 and IleH11 and from now on called short tunnel G8 (STG8) as shown schematically in Figure 1(b). In *Mt*-TrHbO TrpG8 is blocking the STG8, and a short tunnel with a lower barrier for ligand migration is found in the opposite direction towards E7 (STE7). Interestingly in *Mt*-TrHbO, the TrpG8 is also responsible for blocking the LT and therefore key for ligand entry.[8,9] In *Mt*-trHbN the LT opening is controlled by PheE15, which acts as a gate for ligand migration. It is worth noting that the TrpG8 is conserved on the whole Group II and III, but it is not found in group I TrHb.

The case of truncated hemoglobin O of *B. subtilis* (*Bs*-trHbO) is, nevertheless, a challenging system, as the structural features of this protein do not permit to rationalize the ligand binding properties. Although TrpG8 is present in *Bs*-TrHbO, and therefore both LT and STG8 are expected to be blocked, the ligand association rate k_{on} is higher than that found for *Mt*-trHbO, and surprisingly similar to that correspond to

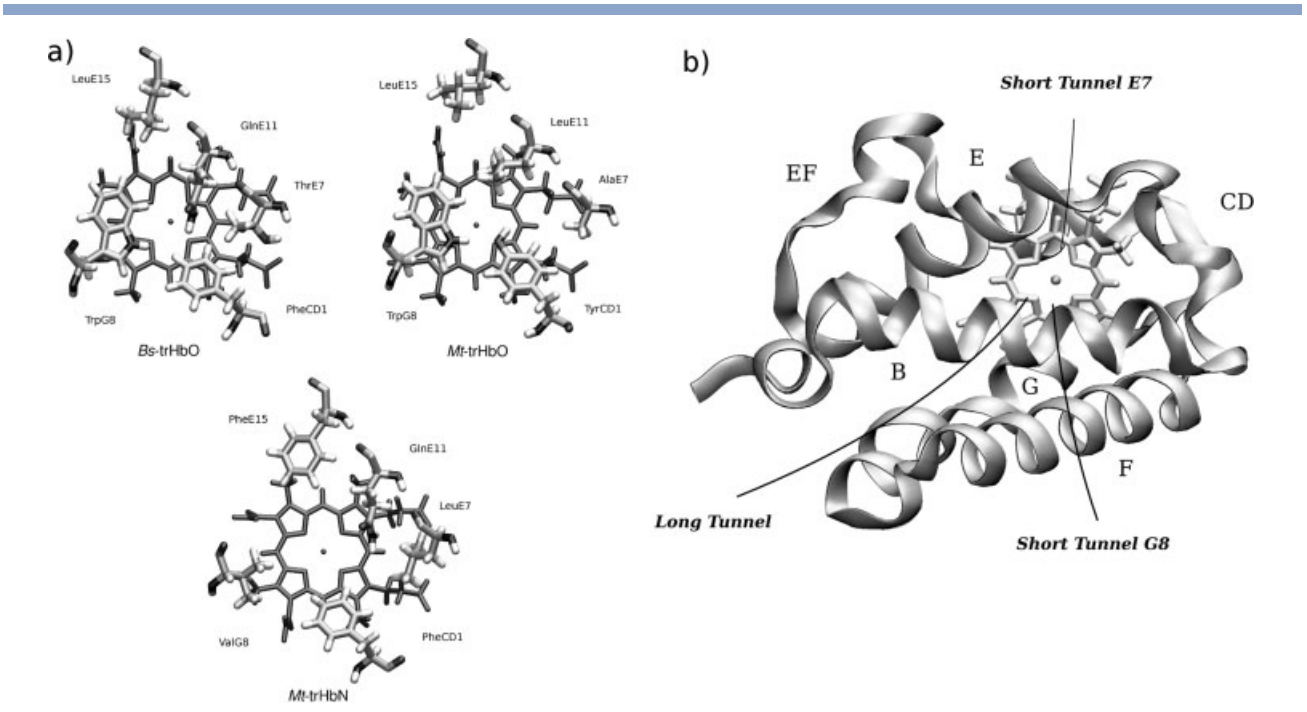

Figure 1

a) Active site of three different truncated hemoglobins: *B. subtilis* truncated hemoglobin O (*Bs*-trHbO), *M. tuberculosis* truncated hemoglobin O (*Mt*-trHbO), *M. tuberculosis* truncated hemoglobin N (*Mt*-trHbN). **b**) Schematic representation of the Long (LT), Short E7 (STE7), and Short G8 (SG8T) tunnels for ligand migration in the tertiary structure context of *Bs*-trHbO.

Table I
Kinetic Data of Three Different Truncated Hemoglobins

Heme-protein	$k_{on}O_2 \times (M^{-1}\ s^{-1})$	$k_{off}\ O_2 \times (s^{-1})$
Bs-trHbO [12]	1.4×10^7	2.1×10^{-3}
Mt-trHbO [4]	1.1×10^5	1.4×10^{-3}
	8.5×10^5	5.8×10^{-3}
Mt-trHbN [5]	2.5×10^7	2.0×10^{-1}

B. subtilis truncated hemoglobin O (Bs-trHbO) (12), *M. tuberculosis* truncated hemoglobin O (*Mt*-trHbO) (4), *M. tuberculosis* truncated hemoglobin N (*Mt*-trHbN) (5).

Mt-trHbN (Table I). On the other hand, *Bs*-tr7HbO has three residues (TrpG8, TyrB10, and GlnE11) capable of interacting with the bound ligand,[12] but as the X-ray structure corresponds to the CN state, the details of the HB network in the physiologically oxygenated protein are unknown.

In this study, we have performed computational simulations of wild type and selected mutant *Bs*-TrHbO to understand the structural determinants of its ligand binding properties at the atomic level. To elucidate the potential implication of different tunnels in ligand binding migration, we performed molecular dynamics simulation (MD) of the protein in the deoxygenated state and computed the free energy profile for ligand migration along each tunnel. On the other hand, MD simulations of the oxygenated and carboxygenated protein were performed to shed light on the role of the HB network on ligand binding, and its connection with kinetic properties.

METHODS

MD simulations were performed starting from the crystal structure of wild-type cyano-met *Bs*-trHbO, solved at 2.1 Å resolution (PDB entry: 1ux8.pdb).[12] The CN^- was replaced for an O_2 or CO ligands. The system was then immersed in a box of TIP3P water molecules of 2985 water molecules.[13] The minimum distance between protein and wall was 12 Å. All systems were simulated employing periodic boundary conditions and Ewald sums for treating long range electrostatic interactions.[14] Shake was used to keep bonds involving H atom at their equilibrium length. This allowed us to employ a 2 fs time step for the integration of Newton's equations. The parm99 and TIP3P force fields implemented in AMBER were used to describe the protein and water, respectively.[15] The oxygenated and carboxygenated heme model system charges were determined as described in previous works[7] (Supporting Information). The temperature and pressure were regulated with the Berendsen thermostat and barostat, respectively, as implemented in AMBER.

All systems were minimized to optimize any possible structural clashes. Subsequently, the systems were heated slowly from 0 to 300 K using a time step of 0.1fs, under constant volume conditions. Finally, a short simulation at constant temperature of 300 K, under constant pressure of 1 bar was performed using a time step of 0.1fs, to allow the systems to reach proper density. These equilibrated structures were the starting point for production MD simulations.

Mutations were performed *in silico* by changing the corresponding amino acid in the original structure, and allowing the system to equilibrate as mentioned earlier.

Migration free energy profiles

To examine the properties of the hydrophobic tunnels in *Bs*-trHbO from *B. subtilis*, the migration free energy profiles were determined in deoxygenated state of the protein. Free energy profiles were determined by means of constant velocity multiple steered molecular dynamics (MSMD) simulations, and using the Jarzynski's equality,[16] which relates the equilibrium free energy (ΔG) along the reaction coordinate with the irreversible work performed over the system when it is steered along the coordinate at constant temperature according to:

$$\exp[-\Delta G(\xi)/k_b T] = \langle \exp[-W(\xi)/k_b T] \rangle$$

where $W(\xi)$ is the external work performed on the system as it evolves from the initial to the final state along the reaction coordinate (ξ), computed by integrating the force acting on the steering potential along ξ.

The steering potential "$E(r)$" is a harmonic well that moves with constant velocity (v) along the reaction coordinate:

$$E(r) = k[r - (\xi_o + v\Delta t)]^2$$

The reaction coordinate ξ was chosen as the iron–ligand distance. The force constant used was 200 k cal/mol Å. The pulling velocity used was 0.025 Å/ps. To construct the free energy profile of ligand migration along a selected tunnel, a set of independent MSMD simulations were performed, in which the ligand was pulled from the solvent to the active site. Every set of MSMD runs was performed starting from equilibrated MD structures, corresponding with the ligand in different internal places of the protein: Entrance of tunnel, or local minimum. To decrease the error of MSMD simulations, we performed each MSMD in a maximum range of 6 Å (Supporting Information).

In practice, to construct the free energy profile of ligand migration along a selected tunnel stretch (from minima to minima) 40 individual MSMD simulations were performed. Every MSMD run was performed start-

ing from a different equilibrated structure, with the ligand located in the corresponding secondary docking site or at the entrance of tunnel (i.e in the solvent). The resulting individual work profiles were combined to compute the corresponding free energy profile. The complete profile along the whole tunnel length was then built by joining the segment profiles.

Convergence of each profile was determined by computing different exponential averages, each using an increasing number of individual work profiles, until no significant changes in the resulting profile were obtained with the incorporation of new work profiles. This is nicely shown in Figure SIF8–SIF13, where free energy profiles computed using 10, 15, 20, 25, 30, 35, and 40 individual MSMD simulations are depicted. As can be seen after 20–30 MSMD simulations, the resulting free energy profile does not change significantly due to the addition of new simulations. The relatively small number of MSMD required to achieve convergence in the computer free energy profiles is due to the fact that the ligand migration process does not imply significant protein reorganization.

This computational scheme has been successfully applied to compute the free energy profile of ligand migration in *Mt*-trHbN and *Mt*-trHbO and also to compute free energy profiles of enzymatic reactions.[9,10,17]

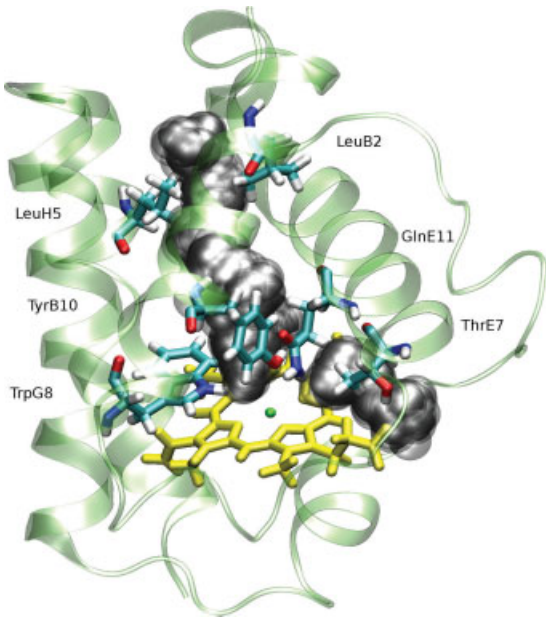

Figure 2

View of the truncated hemoglobin O of *B. subtilis* (*Bs*-trHbO). The heme group is depicted in yellow, the relevant residues are shown in light blue, and the long and short tunnel are depicted in gray.

RESULTS

Simulation stability

To evaluate the stability of the simulations, and to corroborate the correct thermalization of the different systems studied, we have plotted the RMSD of the protein vs time of simulation. The results show that all simulations (wild type and different mutant proteins) are stable and equilibrated after a few nanoseconds (Supporting Information). Comparison of the MD representative structures with the original crystal structure shows no significant changes in the overall structure (CA–CA distance is less than 1 Å). Also, the comparison of MD fluctuations with the experimental B-factor shows that the simulation accurately represents the flexible and/or rigid zones of the tertiary structure obtained experimentally (Supplementary Information: Figures 14 and 15).

Detection of possible tunnels for ligand migration

Two different strategies were used to characterize internal tunnels for ligand migration. First, several MD simulation of the free protein with unbound ligand initially located into the distal side of the heme cavity were performed. Then, free energy profiles for each possible tunnel were determined.

The results obtained from MD simulation show that, although the X-ray structure does not show a clear tunnel for ligand migration, two possible tunnels could be identified as plausible pathways for ligand migration, which correspond to typical LT and STE7, respectively, as noted in Figure 2.

To establish the relevance of each tunnel and to characterize them from a thermodynamic viewpoint, we computed the free energy profiles for O_2 migration using MSMD computations. For the LT [Fig. 3(a)], migration can occur with almost no barrier. The ligand is initially trapped in cavity at about 11 Å from the iron, and from there only a very small barrier (less than 1 k cal/mol) must be surpassed to access the distal cavity at about 6 Å from the iron. The largest barrier (about 2 k cal/mol) for ligand migration towards the heme cavity is located at the entrance of the LT, and can be ascribed to the interaction of the ligand with four Leu residues: LeuB2, LeuB5, LeuE15, and LeuH5 (Fig. 2).

The results for the STE7 [Fig. 3(b)] show that the tunnel displays a high barrier for ligand migration from the solvent into the heme active site. Residues involved in the energetic barrier are probably ThrE7 and GlnE11. Therefore, the results suggest that ligands will enter into the protein through the LT, and this migration will occurs without a significant hindrance.

As mentioned in the introduction, in *Mt*-TrHbO TrpG8 blocks the LT resulting in a barrier larger than 10 kcal/mol for ligand entry into the protein. In this case,

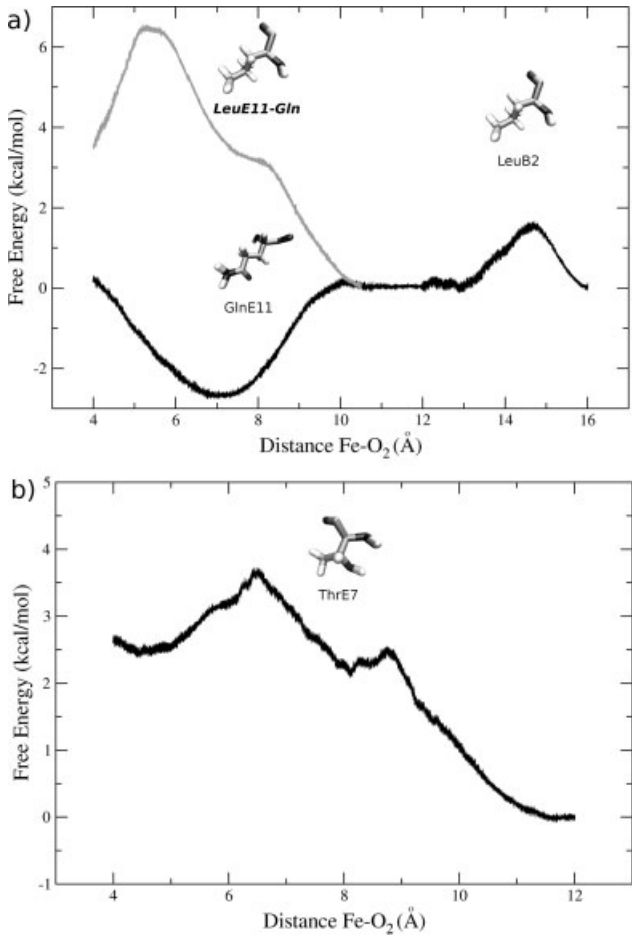

Figure 3

a) Free energy profiles for ligand migration through the long tunnel. Results for the wild type and mutant GlnE11-Leu are shown in black and grey lines, respectively. **b**) Free energy profile for ligand migration through short tunnel E7 in wild type protein.

although the same residue TrpG8 is present in *Bs*-TrHbO access to the heme cavity is not limited by a relevant barrier for this protein. This difference can be attributed to residue E11, which is Leu in *Mt* and Gln in *Bs*. In *Bs*-trHbO the O atom of GlnE11 is bound to TyrB10 hydroxyl hydrogen, generating the rotation of GlnE11 towards the tyrosine. This motion of GlnE11 leads to a tunnel free for ligand migration, and blocks the STE7.

To determine if the motion of GlnE11 is responsible for the low barrier, the GlnE11-Leu mutant was built up *in silico* and the corresponding free energy profile for ligand migration was determined. The results [Fig. 3(a)] reveal that this mutant protein presents a higher barrier for ligand migration when compared to the wild type protein, which supports the hypothesis about the relevant contribution of residue E11 to modulate the migration of ligands through the LT. Overall, during ligand migration through any of the tunnels, protein structure remains unchanged and only local sidechain motions as those described earlier are observed.

Analysis of distal cavity HB network

Oxy wt-BsTrHbO

A 20 ns MD simulation was performed to analyze the structure of the distal cavity in the oxy *Bs*-TrHbO. Initially, TrpG8 and TyrB10 occupy the same position found in the X-ray structure while GlnE11 moves towards TyrB10 forming an HB between its amide carbonyl-O and TyrB10-OH [Fig. 4(a)]. This interaction allows the amide NH2 group of GlnE11 to be hydrogen bonded with O_2 with bond distance of 2.32 $\pm$ 0.42 Å. This HB pattern remains for about 3ns [Fig. 4(c,d)], after which the HB between GlnE11 and O_2 is broken and the amide moiety forms a new HB with the hydroxyl oxygen of TyrB10, which in turn is HB to the coordinated oxygen (bond distance of 2.06 $\pm$ 0.27 Å) [Fig. 4(b)]. During the whole simulation time TrpG8 is forming a strong HB with O_2 (bond distance of 2.07 $\pm$ 0.24 Å). As no shift to the original conformation of GlnE11 is observed during the rest of the simulation time, the initial HB pattern probably represents a bias due to the initial CN bound crystal structure, while the final stable structure represents the actual oxy stable conformation of the protein.

Based on the preceding analysis, it is clear that two strong HB are established with the heme-bound O_2. This behavior is similar in *Mt*-trHbO, where one of the residues is TrpG8 and the other is TyrCD1 (data not shown).[4] As in both proteins (*Bs*-trHbO and *Mt*-trHbO) there are two residues stabilizing the heme-bounded O_2, and one of the residues is TrpG8, which is forming a strong HB, is not surprising that the *koff* was similar in both proteins

Oxy TrpG8 to Leu BsTrHbO

As mentioned in the Introduction, TrpG8 forms a strong HB with heme-bound O_2 in *Mt*-TrHbO, which contributes to the low *koff* in this protein. To determine the relevance of the TrpG8 on the HB network in *Bs*-TrHbO, the TrpG8-Leu mutant protein was examined by means of a 20ns MD simulation. The analysis of the trajectory reveals that when Trp is removed, TyrB10 establishes a strong HB with the bound O_2 (bond distance of 2.04 $\pm$ 0.29 Å), while GlnE11 is hydrogen-bonded to TyrB10 (bond distance of 2.28 $\pm$ 0.41 Å), similar to the wt protein (Supporting Information Figure SIF16). Comparison of HB for wt and mutant protein are shown in Figure 5. Accordingly, the mutation TrpG8-Leu should diminish the number of HB with O_2, and therefore the *koff* should increase.

CO bound Wt-BsTrHbO

In the last years, several groups have performed MD simulations to understand the Resonance Raman

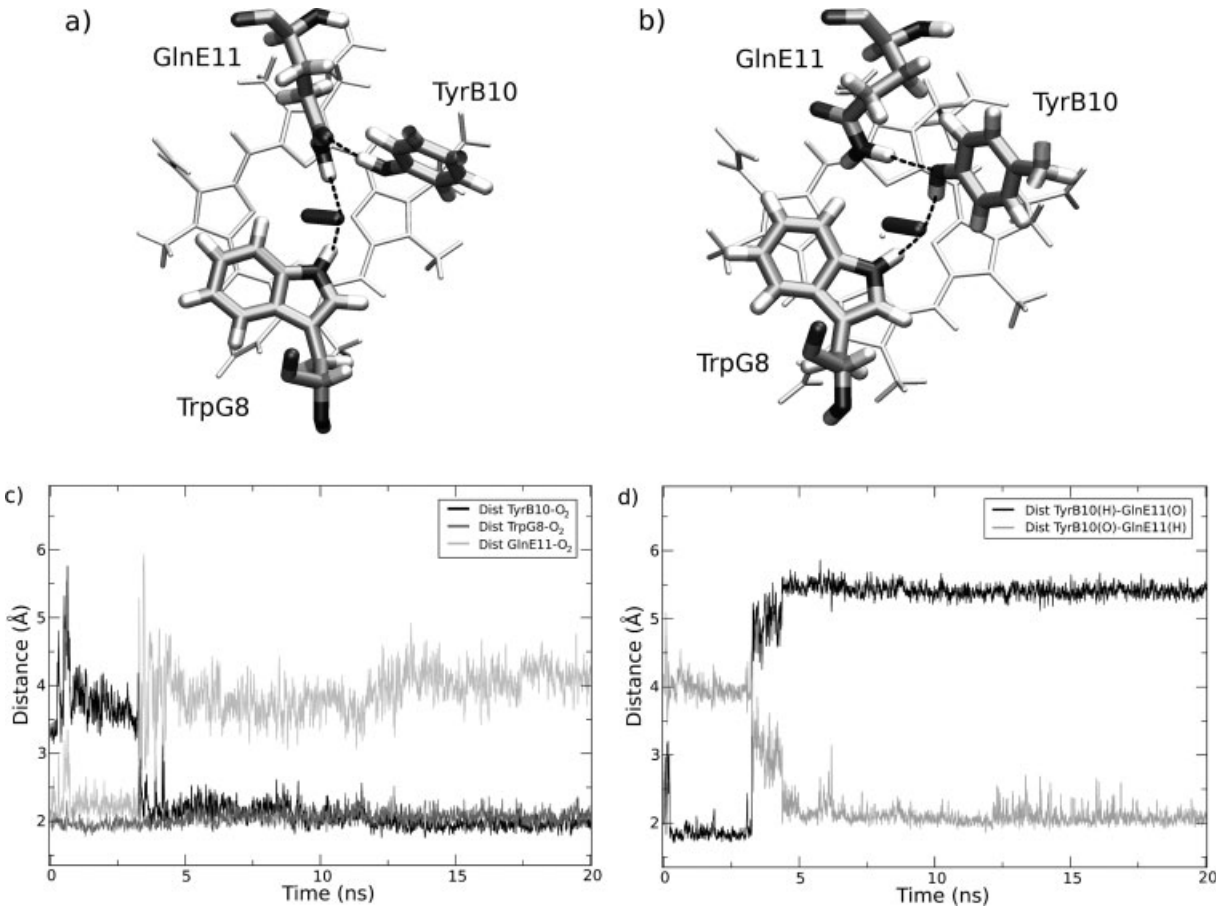

Figure 4

Schematic representation of the neighboring location of wild type *Bs*-trHbO distal site with O_2, showing the residues of the HB network. **a**) GlnE11 and TrpG8 form HBs with the ligand, and TyrB10 is hydrogen-bonded to GlnE11. **b**) The second conformation of the protein, where TyrB10 and TrpG8 form HB with the coordinated dioxygen. In this case it can be observed the HB between GlnE11 and TyrB10. **c**), **d**) Time evolution of selected distances among distal residues and the coordinated O_2. TyrB10-O_2, TrpG8-O_2, and GlnE11-O_2 distances are depicted with black, grey, and light grey lines, respectively. d) Time evolution of selected distance between distal residues TyrB10-GlnE11.

experiments.[18,19] The availability of Resonant Raman data for *Bs*-trHbO (discussion) prompted us to examine the structure and dynamics of CO bound in *Bs*-trHbO by means of MD. Our results show that there exist two conformations depending on the motion of the GlnE11 and the TyrB10 (Fig. 6). As noted for the oxygenated protein, in the first conformation a HB is formed between CO and distal residues TrpG8 and GlnE11 [Fig. 6(a)]. Moreover, the hydroxyl group of TyrB10 is also hydrogen-bonded to the amide-carboxyl of GlnE11. In the second conformation, however, the situation is different from the one observed in the oxy protein. In this case TyrB10 remains hydrogen-bonded to GlnE11, but this residue is no longer hydrogen-bonded to CO and moves away strengthening its interaction with TyrB10 [Fig. 6(b)]. For these reasons, in this conformation the heme-bound CO has only one hydrogen bond. Both structures are in dynamic equilibrium as shown by the distance plot [Fig. 6(c)], population analysis shows that the HB between GlnE11 and bound CO corresponding to conformation 1 is present about 35% of the simulation time. The HB distances between coordinated CO and TrpG8 and GlnE11 are 2.18 ± 0.25 Å, and 2.91 ± 0.63 Å, respectively.

CO bound TrpG8Leu Bs-TrHbO

As in the case of heme-bound O_2, the simulation of TrpG8-Leu mutant presents only one conformation, where TyrB10 is hydrogen-bonded to CO (bond distance of 2.19 ± 0.33 Å), whereas GlnE11 is only interacting with OH of TyrB10. (Supporting Information Figure SIF17 for details)

DISCUSSION

Truncated hemoglobins (TrHbs) are a large sub family of proteins, which has been intensively studied in the last

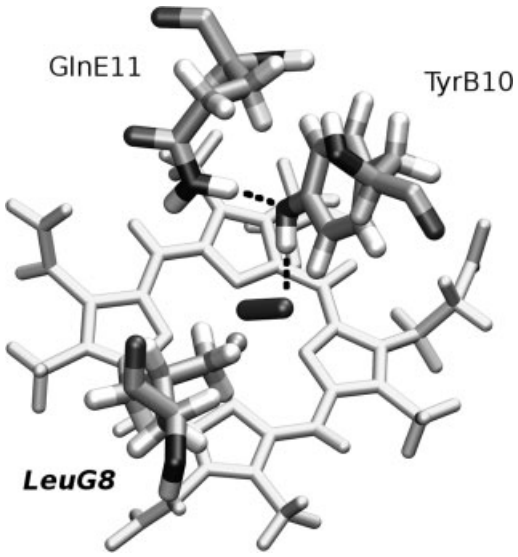

Figure 5

Schematic representation of the neighboring location of TrpG8-Leu mutant *Bs*-trHbO distal site with O_2, showing the residues involved in the HB network.

decade, due to its interesting structural and ligand binding properties. The most striking features are the presence of extensive tunnel cavity systems that connects the solvent to the heme-active site, and the complex HB network displayed in the distal cavity that modulates ligand affinity and ligation linked conformational dynamics.[1,10]

Bs-TrHbO is the second protein structurally characterized from group II, and presents several interesting features that motivated this study. The most striking feature of the members of the group II is the lack of the short tunnel G8 (STG8), due to the presence of TrpG8. In the case of *Mt*-trHbO, the TrpG8 also blocks the LT, making short tunnel E7 (STE7) to be the only possible pathway for the ligand migration. The case of *Bs*-TrHbO is more complex, as the presence of a threonine residue at position E7 typically blocks STE7. Therefore, the X-ray crystallographic structure does not exhibit a clear tunnel for ligand migration. However, its kinetic constants k_{on} were very high to assume the lack of those tunnels. Indeed, this kinetic constant is similar to *Mt*-trHbN one, which presents a clear tunnel in the X-ray structure.

Using MD simulations and MSMD, we have shown that the LT in *Bs*-trHbO is open, as in the case of *Mt*-TrHbN. When we compare the X-ray structure, at about 0.5 ns of simulation time the LT opens due to a motion of GlnE11, which comes closer to TyrB10. This motion leads to a barrier for ligand migration of about 2.5 k cal/mol, which is consistent with the k_{on} rate constant of 1 10^7 M^{-1} s^{-1}. Noteworthy, the new position of the GlnE11 is similar to that observed in the X-ray crystal structure of the trHbN.[11] Interestingly, the motion of GlnE11 towards TyrB10 not only opens LT, but it closes the STE7 (Fig. 1). Therefore, it seems that ThrE7 and GlnE11 are responsibles for the high barrier found in the ligand migration through STE7.

Comparing *Bs*-trHbO, *Mt*-trHbN, and *Mt*-trHbO; the O_2 association rate constants are similar in the first two cases ($\sim 10^7$ M^{-1} s^{-1}) while it is significantly smaller in the latter case ($\sim 10^5$ M^{-1} s^{-1}). This can be ascribed to the fact that the LT and STG8 are accesible for ligand migration in *Bs*-trHbO and *Mt*-trHbN, respectively; while in *Mt*-trHbO only the more hindered STE7 is open as both LT and STG8 are blocked by TrpG8. On the other hand, the TrpG8 residue does not block the LT in *Bs*-trHbO, as it is generally assumed by inspection of the crystal structure, due to a rearrangement in the distal site involving GlnE11. At this point it is worth noting that in *Bs*-trHbO the LT is open due to the lack of the bulky PheE15, which is acting as a tunnel gate in *Mt*-trHbN.

To corroborate the role of GlnE11, the GlnE11-Leu mutant was examined. Similarly to what is observed in *Mt*-TrHbO, the results show that in this case the tunnel is blocked due to a bottleneck formed between TrpG8 and LeuE11.

Therefore, we can conclude that in group II TrpG8 blocks STG8, and both TrpG8 and LeuE11 block the LT.

Concerning the distal HB network, our results show that in the oxygenated protein two different conformations coexist in the protein. In both cases two residues are forming HBs with the coordinated ligand: TrpG8 and GlnE11 or TrpG8 and TyrB10. However, in the mutant TrpG8-Leu, only TyrB10 is hydrogen-bonded to O_2, and a higher dissociation rate constant *koff* is expected for this mutant protein.

Different results are observed for heme-bound CO. Although there are two different conformations, one of them is different compared to those observed in the oxygenated protein. Thus, TrpG8 is the only residue HB to CO, but TyrB10 and GlnE11 are HB to each other and far away from the ligand in one conformation, while in the other conformation CO exhibits two Hbs with TrpG8 and GlnE11. These results are consistent with the RR results, in which two frequencies for the wild type *Bs*-trHbO protein were observed with CO[20] (Table II).

Regarding the general structure function relationship in TrHbs our results not only reconcile the structural data with the kinetic binding properties, they also give further support to the hypothesis that the LT is the most important in regulating ligand entry in TrHbs. Furthermore, our results shed additional light on the role played by TrpG8, that is conserved in groups II and III. Based on previous data for *Mt*-TrHbO, the presence of TrpG8 seemed to impose a big constrain to ligand migration as it was able to block both LT and STG8. The data presented here show once more the plasticity and redundancy of several residues of the globin fold to account for ligand binding kinetics. Although the presence of

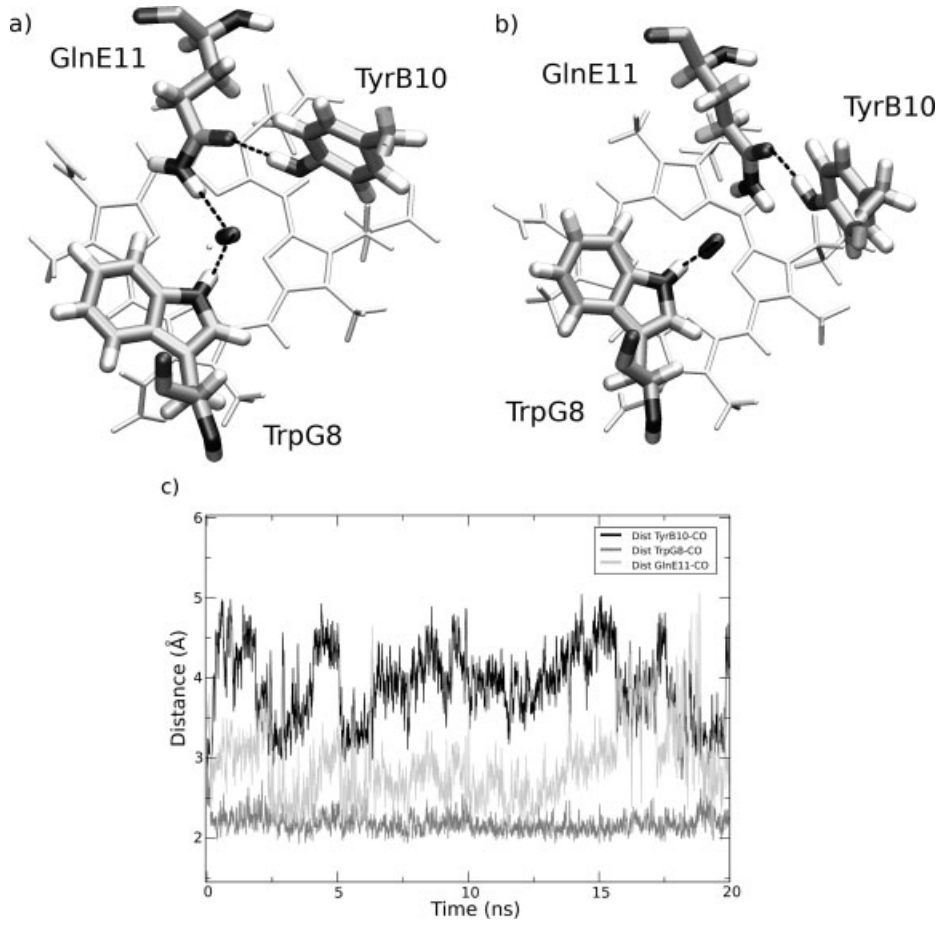

Figure 6

Schematic representation of the wild type *Bs*-trHbO distal site with CO, showing the residues of the HB network. **a**) in the first conformation GlnE11 and TrpG8 are hydrogen-bonded with the ligand, and the TyrB10 forms an hydrogen bond with GlnE11. **b**) In the second conformation TyrB10 and TrpG8 are hydrogen-bonded to CO, and GlnE11 interact with TyrB10. **c**) Time evolution of selected distances among distal residues and the coordinated CO. TyrB10-CO, TrpG8-CO, and GlnE11-CO distances are depicted with black, grey, and light grey lines, respectively.

TrpG8 was expected to hinder ligand entry, the presence of a Gln in position E11, compared to Leu found in *Mt*-TrHbO clearly opens up the LT allowing ligand entry and resulting in fast association rates. Interestingly, analysis of all TrHbOs sequences shows that this residue is either Leu or Gln, with similar frequencies, Phe in about five cases and Ser in two cases. Based on our data a Phe is expected to also display a very closed channel, while a Ser may lead to an open channel. In this view the TrHbOs can be divided in those displaying LT open when Gln/Ser in position E11 and those closed when Leu/Phe is found. Furthermore, the phylogenetic tree of GroupII TrHbs shows a first division completely correlated with the presence of Leu/Phe or Gln in position E11 (proteins with a Ser in E11, belong to a separate cluster). The fact that the predicted open or closed LT state is correlated with the protein phylogenetic analysis points out that this position may be a key in regulating TrHb properties and therefore its function, therefore conditioning evolution in other positions.

Table II

Resonant Raman Vibrational Frequencies (cm^{-1}) For *B. subtilis* Truncated Hemoglobin O (*Bs*-trHbO) (20)

	ν(FeC)	ν(CO)
Bs-trHbO (CO)	545	1888
	520	1924
Bs-trHbO-WG8L (CO)	524	1920
	489	1958

ACKNOWLEDGMENTS

We thanks to Dr Pablo De Biase for his many useful contributions. The simulation were performed in the Marenostrum supercomputer in Barcelona, and in the C.EC.A.R. in Buenos Aires.

REFERENCES

1. Milani M, Pesce A, Nardini M, Ouellet H, Ouellet Y, Dewilde S, Bocedi A, Ascenzi P, Guertin M, Moens L, Friedman JM, Wittenberg JB, Bolognesi M. Structural bases for heme binding and diatomic ligand recognition in truncated hemoglobins. J Inorg Biochem 2005;1:97–109.
2. Wittenberg JB, Bolognesi M, Wittenberg BA, Guertin M. Truncated hemoglobins: a new family of hemoglobins widely distributed in bacteria, unicellular eukaryotes, and plants. J Biol Chem 2002;277: 871–874.
3. Pesce A, Nardini M, Milani M, Bolognesi M. Protein fold and structure in the truncated (2/2) globin family. Gene 2007;398: 2–11.
4. Pathania R, Navani NK, Rajamohan G, Dikshit KL. Mycobacterium tuberculosis hemoglobin HbO associates with membranes and stimulates cellular respiration of recombinant Escherichia coli. J Biol Chem 2002;277:15293–15302.
5. Couture M, Yeh SR, Wittenberg BA, Wittenberg JB, Ouellet Y, Rousseau DL, Guertin M. A cooperative oxygen-binding hemoglobin from *Mycobacterium tuberculosis*. Proc Natl Acad Sci USA 1999; 96:11223–11228.
6. Vuletich DA, Lecomte JT. A phylogenetic and structural analysis of truncated hemoglobins. J Mol Evol 2006;62:196–210.
7. Crespo A, Martí MA, Kalko SG, Morreale A, Orozco M, Gelpi JL, Luque FJ, Estrin DA. Theoretical study of the truncated hemoglobin HbN: exploring the molecular basis of the NO detoxification mechanism. J Am Chem Soc 2005;127:4433–4444.
8. Ouellet H, Milani M, LaBarre M, Bolognesi M, Couture M, Guertin M. The roles of Tyr(CD1) and Trp(G8) in *Mycobacterium tuberculosis* truncated hemoglobin O in ligand binding and on the heme distal site architecture. Biochemistry 2007;46:11440–11450.
9. Boechi L, Martí MA, Milani M, Bolognesi M, Luque FJ, Estrin DA. Structural determinants of ligand migration in *Mycobacterium tuberculosis* truncated hemoglobin O. Proteins 2008;73:372–379.
10. Bidon-Chanal A, Martí MA, Crespo A, Milani M, Orozco M, Bolognesi M, Luque FJ, Estrin DA. Ligand-induced dynamical regulation of NO conversion in *Mycobacterium tuberculosis* truncated hemoglobin-N. Proteins 2006;64:457–464.
11. Milani M, Pesce A, Ouellet Y, Ascenzi P, Guertin M, Bolognesi M. *Mycobacterium tuberculosis* hemoglobin N displays a protein tunnel suited for O_2 diffusion to the heme. EMBO J 2001;20:3902–3909.
12. Giangiacomo L, Ilari A, Boffi A, Morea V, Chiancone E. The truncated oxygen-avid hemoglobin from *Bacillus subtilis*: X-ray structure and ligand binding properties. J Biol Chem 2005;280:9192–9202.
13. Jorgensen WL, Chandrasekar J, Madura J, Impey RW, Klein ML. Comparison of simple potential functions for simulating liquid water. J Chem Phys 1983;79:926–935.
14. Luty BA, Tironi IG, Van Gunsteren WF. Lattice-sum methods for calculating electrostatic interactions in molecular simulations. J Chem Phys 1995;103:3014–3021.
15. Pearlman DA, Case DA, Caldwell JW, Ross WS, Cheatham TE, Debolt S, Ferguson D, Seibel G, Kollman P. AMBER, a package of computer programs for applying molecular mechanics, normal mode analysis, molecular dynamics and free energy calculations to simulate the structural and energetic properties of molecules. Comput Phys Commun 1995;91:1–41.
16. Jarzynski C. Nonequilibrium equality for free energy differences. Phys Rev Lett 1997;78:2690–2693.
17. Crespo A, Martí MA, Estrin DA, Roitberg AE. Multiple-steering QM-MM calculation of the free energy profile in chorismate mutase. J Am Chem Soc 2005;127:6940–6941.
18. Lu C, Egawa T, Mukai M, Poole RK, Yeh SR. Hemoglobins from *Mycobacterium tuberculosis* and *Campylobacter jejuni*: a comparative study with resonance Raman spectroscopy. Methods Enzymol 2008; 437:255–286.
19. Di Lella S, Ma L, Ricci JC, Rabinovich GA, Asher SA, Alvarez RM. Critical role of the solvent environment in galectin-1 binding to the disaccharide lactose. Biochemistry 2009;48:786–791.
20. Feis A, Lapini A, Catacchio B, Brogioni S, Foggi P, Chiancone E, Boffi A, Smulevich G. Unusually strong H-bonding to the heme ligand and fast geminate recombination dynamics of the carbon monoxide complex of *Bacillus subtilis* truncated hemoglobin. Biochemistry 2008;47:902–910.